Mechanism-Based Development of a Low-Potential, Soluble, and Cyclable Multielectron Anolyte for Nonaqueous Redox Flow Batteries

Christo S. Sevov,[†,§] Sydney L. Fisher,[‡,§] Levi T. Thompson,*[‡] and Melanie S. Sanford*[†]

[†]Department of Chemistry, University of Michigan, 930 North University Avenue, Ann Arbor, Michigan 48109, United States
[‡]Department of Chemical Engineering, University of Michigan, 2300 Hayward Street, Ann Arbor, Michigan 48109, United States

Ⓢ Supporting Information

ABSTRACT: The development of nonaqueous redox flow batteries (NRFBs) has been impeded by a lack of electroactive compounds (anolytes and catholytes) with the necessary combination of (1) redox potentials that exceed the potential limits of water, (2) high solubility in nonaqueous media, and (3) high stability toward electrochemical cycling. In addition, ideal materials would maintain all three of these properties over multiple electron transfer events, thereby providing a proportional increase in storage capacity. This paper describes the mechanism-based design of a new class of metal-coordination complexes (MCCs) as anolytes for NRFBs.

The tridentate bipyridylimino isoindoline (BPI) ligands of these complexes were designed to enable multielectron redox events. These molecules were optimized using a combination of systematic variation of the BPI ligand and the metal center along with mechanistic investigations of the decomposition pathways that occur during electrochemical cycling. Ultimately, these studies led to the identification of nickel BPI complexes that could undergo stable charge-discharge cycling (<5% capacity loss over 200 cycles) as well as a derivative that possesses the previously unprecedented combination of high solubility (>700 mM in CH_3CN), multiple electron transfers at low redox potentials (−1.7 and −1.9 V versus Ag/Ag⁺), and high stability in the charged state for days at high concentration. Overall, the studies described herein have enabled the identification of a promising anolyte candidate for NRFBs and have also provided key insights into chemical design principles for future classes of MCC-based anolytes.
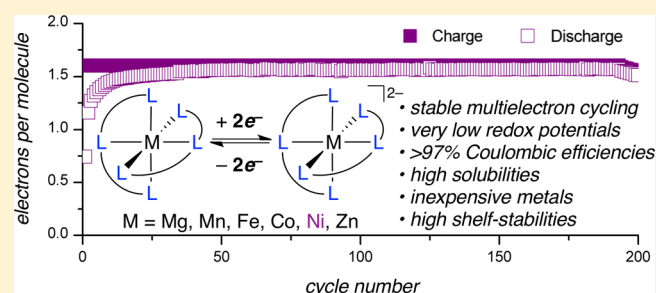
INTRODUCTION

Redox flow batteries (RFBs) are energy storage devices that use solvated redox-active species to interconvert chemical and electrical energy.[1−3] During RFB operation, solutions containing the electroactive species (termed anolytes and catholytes) are pumped from external reservoirs over inert electrodes to charge and discharge the battery.[4,5] In established RFBs, the electroactive species are aqueous solutions of redox-active transition-metal salts or organic molecules.[6−13] Despite many recent advances, the achievable cell voltages in these systems are inherently limited by the small ∼1.5 V electrochemical stability window of the aqueous medium.[5] As such, aqueous RFBs suffer from moderate energy densities and thus require large quantities of solvent, supporting salts, and electroactive compounds to achieve high storage capacity.

In principle, this limitation could be addressed through the development of electrolytes that are compatible with non-aqueous solvents such as acetonitrile, which is electrochemically stable over a 5 V window.[2] Despite their promise, nonaqueous redox flow batteries (NRFBs) remain underdeveloped for two main reasons. First, the separators and cell components employed in aqueous RFBs are incompatible with nonaqueous systems.[14−17] Second (and directly relevant to this paper),

there are currently no electroactive species that possess the properties necessary for this application. Specifically, NRFBs require electroactive molecules with a combination of three features: (1) redox potentials that exceed the potential limits of water, (2) high solubility, and (3) high stability toward electrochemical cycling. Furthermore, ideal materials would maintain these three properties while cycling over multiple redox couples, thereby providing a proportional increase in storage capacity.

Metal-coordination complexes (MCCs) bearing acetylaceto-nate (acac),[18−22] dithiolate,[23,24] 2,2′-bipyridine (bpy),[25−34] and cyclopentadienyl[35−37] ligands have recently gained attention as electrolytes for NRFBs. However, to date, none of these materials possess all three of the features discussed above. For example, ferrocene-based MCCs exhibit high solubility in nonaqueous media as well as stable single-electron electro-chemical cycling. However, their redox potentials are modest (i.e., within the range of aqueous media).[35,37] In contrast, several bipyridine-[33,34] and acac-derived[22,38] MCCs exhibit multiple redox couples over a much wider potential window, as

well as high solubility in nonaqueous media. However, none of these complexes undergo stable electrochemical cycling (typically showing >50% capacity fade after <10 cycles). In these latter systems, the mechanistic origin of the poor cyclability is not well understood, and there have been no systematic evaluations of MCC decomposition pathways during bulk charging. Ultimately, fundamental chemical information about degradation rates and mechanisms are expected to inform the rational design of MCCs that exhibit the combination of cyclability, solubility, and redox potential required for application to NRFBs.

This paper describes the design, synthesis, and electrochemical evaluation of anolyte MCCs bearing tridentate bipyridylimino isoindoline (BPI) ligands (Figure 1). With the
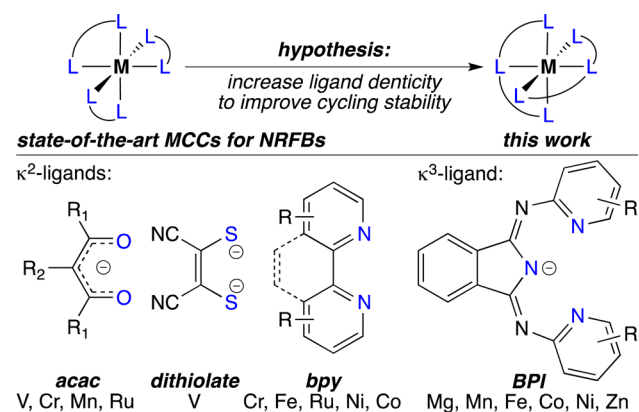

Figure 1. Design strategy of next-generation MCCs for NRFBs.

appropriate selection of ligand substituents and metal center, complexes were identified that exhibit multiple redox couples at very negative potentials as well as high solubility in acetonitrile. Systematic investigations of MCC stability during bulk electrolysis revealed that ligand dissociation is a major degradation pathway. These studies ultimately guided the identification of a highly stable $Ni(BPI)_2$ anolyte that undergoes more than 200 charge–discharge cycles through multiple redox couples at potentials well beyond those of aqueous anolytes.

RESULTS AND DISCUSSION

Ligand Design and MCC Solubility Measurements. Our previous work in this area had focused on developing soluble MCCs that exhibit multiple reversible electron transfers by cyclic voltammetry (CV).[33,34] While promising compounds were identified, these molecules (along with nearly all of the MCCs reported to date) exhibited low stability during charge–discharge cycling in nonaqueous media.[19,20,22,24,25,27,28,34,39] We hypothesized that the poor cyclability of these complexes resulted from dissociation of their bidentate ligands during electrochemical cycling.[40–42] To combat this decomposition pathway, we pursued a tridentate ligand scaffold (BPI, Figure 1), which is expected to bind more strongly to the metal, thereby suppressing ligand dissociation and yielding complexes with enhanced stability and cyclability. MCCs of BPI ligands offer the additional advantage that they undergo reduction at the ligand rather than at the metal.[43,44] As such, these redox-active ligands can serve as reservoirs for multiple electrons and can stabilize the MCCs (since the oxidation state of the metal center remains unchanged during reductive redox processes).

Furthermore, the BPI ligands can be prepared via a modular synthesis, which provides rapid access to a diverse library of complexes (Figure 2a).

We first evaluated the known compound $Ni(L1)_2$ bearing an unsubstituted BPI ligand.[44] As expected for a complex containing a polydentate ligand of high symmetry,[45,46] $Ni(L1)_2$ exhibited extremely low solubility (0.42 mM) in CH_3CN, which precluded CV studies. Our strategy for improving solubility involved decreasing the symmetry of the complexes to disfavor crystal packing[47–50] as well as incorporating alkoxy ether functional groups, which have been shown to enhance the solubility of other MCCs in polar, aprotic solvents (Figure 2b).[22,33] In addition to improved solubility, the BPI derivatives functionalized with electron-donating alkoxy substituents exhibit more negative reduction potentials than the parent MCCs, which is advantageous for applications as anolytes.

The solubilities of nickel complexes $Ni(L1)_2$–$Ni(L6)_2$ were measured in CH_3CN and are summarized in Figure 2c. Modest improvements to solubility were observed upon the incorporation of methoxy substituents [complexes $Ni(L2)_2$ and $Ni(L3)_2$]. Furthermore, derivatives bearing the diethyleneglycoxy (ODG) substituent [complexes $Ni(L4)_2$–$Ni(L6)_2$] exhibited solubility enhancements of more than 3 orders of magnitude versus the parent $Ni(L1)_2$. Most notably, $Ni(L6)_2$ was isolated as a viscous oil that is miscible with CH_3CN to form a free-flowing solution of greater than 700 mM concentration. Moreover, a 250 mM solution of $Ni(L6)_2$ could be prepared in the presence of 500 mM $TBABF_4$, the concentration of supporting electrolyte required for bulk electrolysis.[51] The dramatic effect of minor perturbations of the peripheral ligand structure on solubility is exemplified by the low solubilities of $Ni(L1)_2$–$Ni(L3)_2$, moderate solubilities of $Ni(L4)_2$–$Ni(L5)_2$, and excellent solubility of $Ni(L6)_2$.

We also assessed the impact of metal on MCC solubility using a common ligand framework. Comparative studies were performed on complexes of ligands L4 and L5. These were selected because their Ni complexes are only moderately soluble in CH_3CN (5–15 mM). As such, small perturbations in solubility as a function of metal cation were easier to detect than with other analogues. MCCs of L4 and L5 containing Mg^{2+}, Mn^{2+}, Fe^{2+}, Co^{2+}, Ni^{2+}, and Zn^{2+} were prepared. Single-crystal X-ray structures of the isolated $Mn(L4)_2$, $Fe(L4)_2$, $Ni(L4)_2$, and $Zn(L4)_2$ derivatives show pseudo-octahedral geometries with nearly identical unit cells (see the Supporting Information). Although these complexes are nearly indistinguishable in the solid-state, their solubilities vary from 28 to 8 mM (Figure 2d). A similar trend was observed for complexes of L5, for which the Zn and Ni complexes were less soluble than the Mn and Fe analogues by nearly an order of magnitude. The impact of the metal center on the solubility of this MCC series can be rationalized on the basis of the extent of charge shielding by the ligand.[52] Shielding of the metal ion is typically weaker for early versus late transition metals.[53] As a result, MCCs of earlier metals are expected to be more polar and thus exhibit higher solubility in polar solvents like CH_3CN.

Cyclic voltammetry (CV). We next evaluated the $M(L5)_2$ series via CV in CH_3CN.[54] Each complex exhibits two quasi-reversible reductions at approximately −1.7 and −1.9 V vs Ag/Ag^+ (Figure 3). These occur at nearly identical redox potentials for all of the MCCs, regardless of the metal center, which is consistent with reduction involving a ligand-based orbital. Coulometry experiments confirm that each couple corresponds to a single electron transfer. Voltammetry to positive potentials
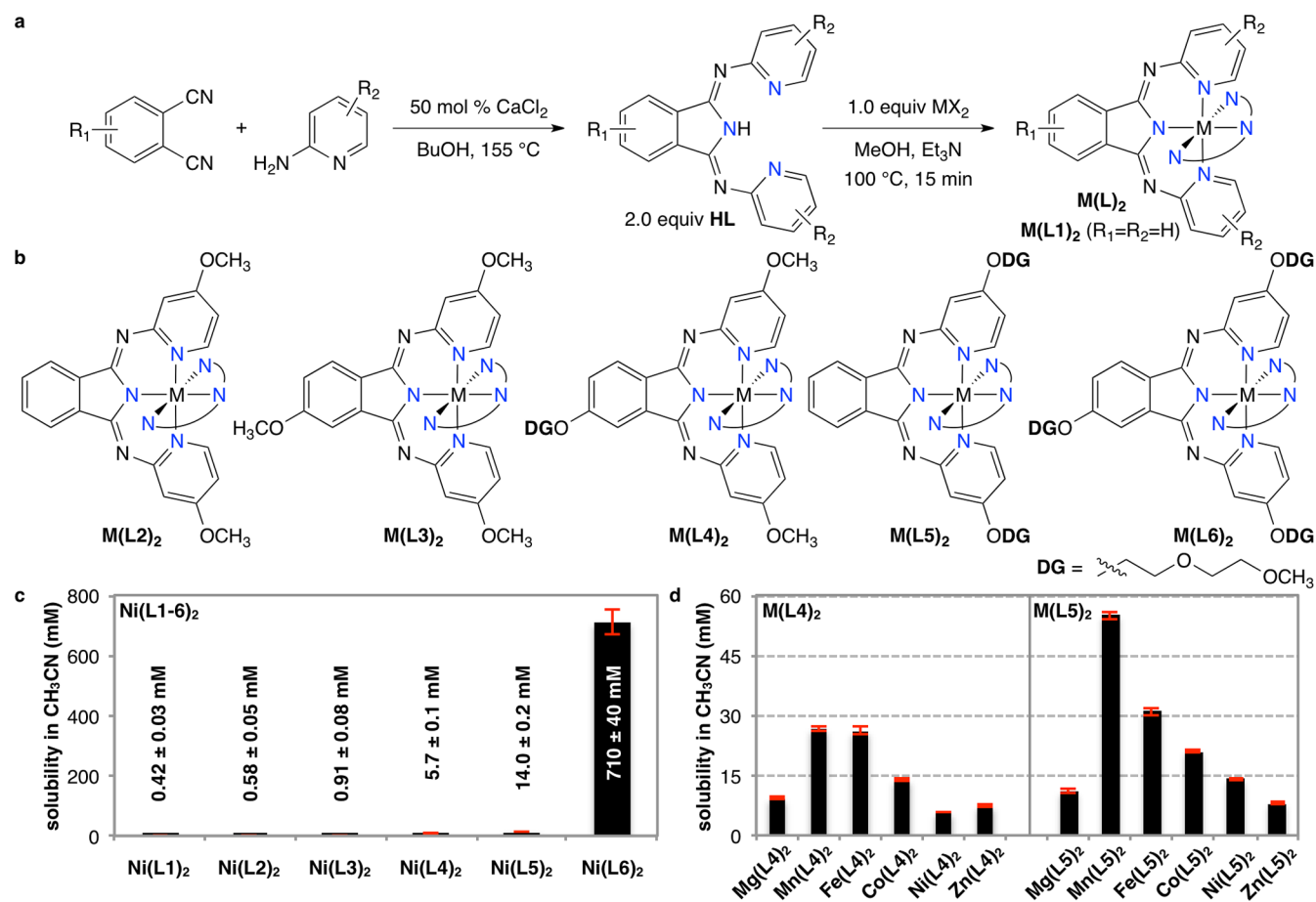
Figure 2. (a) General procedure for the modular synthesis of BPI ligands and their metalation. (b) Prepared MCCs of BPI derivatives with varying metals. (c) Effect of the ligand on the solubility of Ni complexes **Ni(L1)₂**−**Ni(L6)₂**. (d) Effect of the metal center on the solubility of complexes with ligand **HL4** (left) or **HL5** (right).
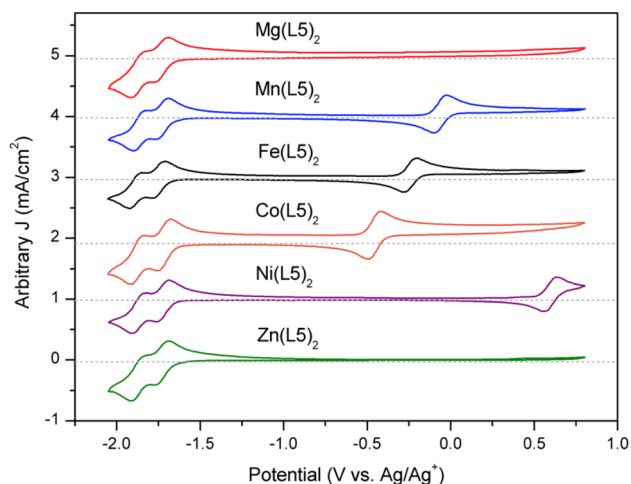

Figure 3. Cyclic voltammograms of **M(L5)₂** analogues. CV conditions: 2 mM M(L5)₂ in CH₃CN with 0.5 M TBABF₄ at 100 mV/s scan rate. Gray dashed lines represent the axis of origin.

revealed quasi-reversible redox couples for **Mn(L5)₂**, **Fe(L5)₂**, **Co(L5)₂**, and **Ni(L5)₂** at varying potentials. These redox processes are consistent with metal-based M^{2+}/M^{3+} oxidations. As expected, no analogous couples at positive potentials were observed for complexes of metals that have filled valence shells [e.g., **Mg(L5)₂** and **Zn(L5)₂**].

Bulk Electrolysis. While the solubility and CV data suggest that the BPI MCCs are promising anolyte candidates, bulk cycling is required to assess their electrochemical stability. To this end, galvanostatic charging and discharging of the **M(L5)₂** series was performed in a glass H-cell with an ultrafine glass frit as the separator. A representative data set for **Zn(L5)₂** is shown in Figure 4. Voltage cutoffs were selected on the basis of CV (Figure 4a) to ensure that only the desired redox couples were accessed. Charge/discharge cycling was performed through two negative redox couples to 100% state-of-charge (SOC) at 1C (0.54 mA) using 2 mM solutions of the MCCs. The potential curve (Figure 4b) during charging exhibits two plateaus (I and II) that are consistent with the redox potentials measured by CV. Discharge occurs with a high voltaic efficiency (90%) at plateaus III and IV. The average Coulombic efficiency (CE) is 94 ± 3%, with minor losses likely resulting from degradation and/or crossover of the charged material through the glass frit. Higher CE (97%) was observed using a faster charge rate (2C), which is likely due to the reduced time for degradation and/or crossover of the charged species.

We next systematically assessed the features that contribute to the charge/discharge stability of M(BPI)₂ complexes. Although reduction of the MCCs is proposed to occur at a ligand-based orbital, variation of the ligand had minimal impact on the cycling profiles of these MCCs (see the Supporting Information). In marked contrast, the identity of the metal had a profound effect (Figure 4d). For example, the filled shell
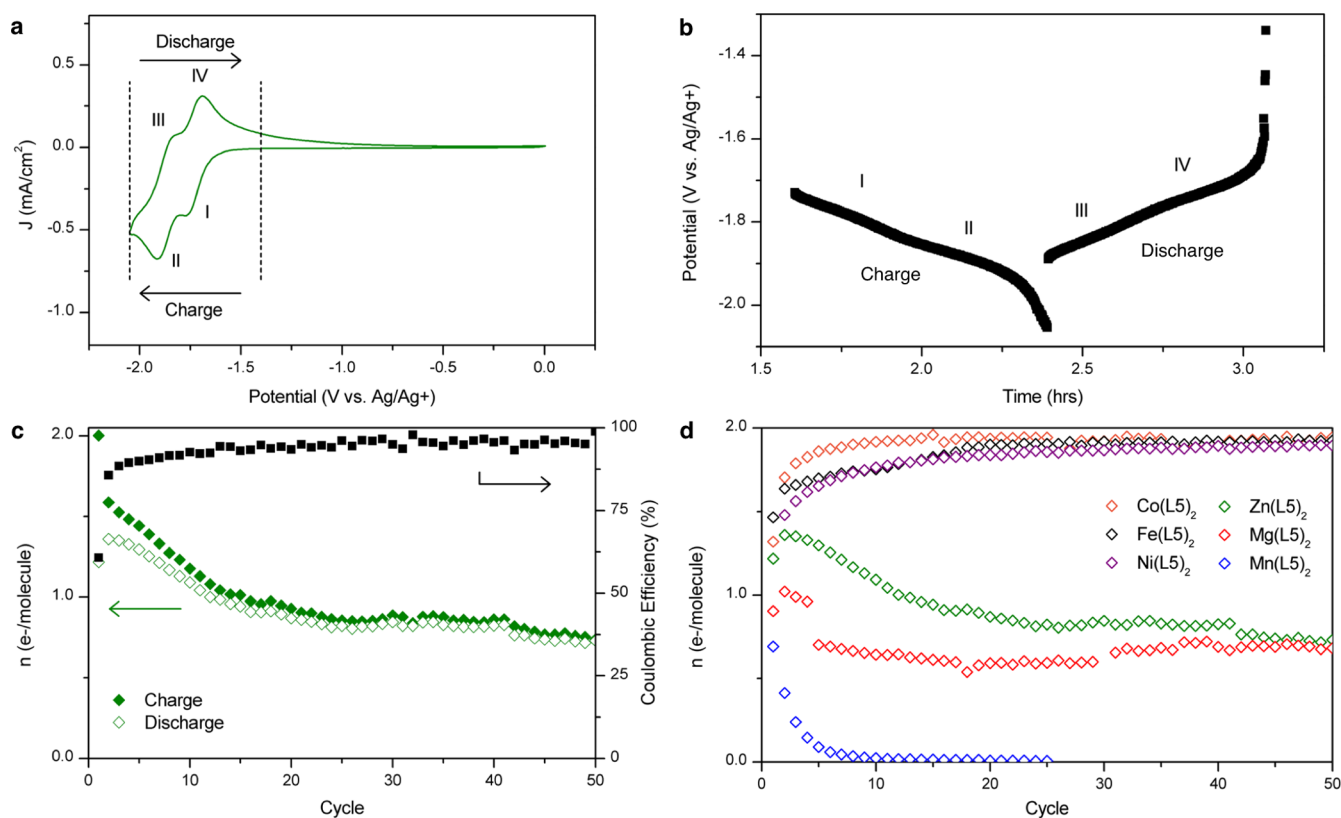
Figure 4. (a) CV of $Zn(L5)_2$. Dashed lines represent the cutoff potentials during bulk cycling. (b) Potential curves for cycle 2 of $Zn(L5)_2$ with charge and discharge plateaus labeled I−IV for comparison to the CV half-wave potentials. (c) Charge and discharge capacities for $Zn(L5)_2$ along with Coulombic efficiency as a function of cycle. (d) Discharge capacity, normalized to the theoretical number of electrons charged, for each complex in the $M(L5)_2$ series.

complexes $Zn(L5)_2$ and $Mg(L5)_2$ showed modest stability (~50% decomposition over 50 cycles). The early-transition-metal complex $Mn(L5)_2$ showed extremely rapid fade of energy storage capacity (complete decomposition in less than 10 cycles). In contrast, complexes of the later transition metals $Ni(L5)_2$, $Co(L5)_2$, and $Fe(L5)_2$ exhibited no detectable loss of storage capacity over 50 charge−discharge cycles to 100% SOC through two electrons. *To our knowledge, these complexes represent the first examples of stable, multielectron cycling of MCC electrolytes for NRFBs.* The dramatic variation in stability as a function of metal is particularly noteworthy because (i) the negative redox events are believed to be solely ligand-based and (ii) these complexes exhibit nearly identical electrochemical behavior at negative potentials when evaluated by CV.

Degradation Mechanisms. To gain further insight into the decomposition pathways, CVs of the relatively unstable Zn and Mg complexes were measured before (dashed traces) and after (solid traces) 25 bulk electrolysis cycles. After cycling, both CVs exhibit an irreversible oxidation at approximately +0.5 V (Figure 5a). It is highly unlikely that this new peak results from a metal-based oxidation of a decomposed Mg^{2+} or Zn^{2+} species.[55] Instead, we hypothesize that it involves oxidation of the free ligand or a fragment thereof.

Ligand shedding is a possible pathway to generate new redox-active species. The immediate organic product of ligand dissociation under the anhydrous conditions of bulk electrolysis would be anionic $L5^-$ with a TBA^+ (TBA = tetrabutylammonium) counterion derived from the supporting electrolyte. To generate an authentic sample of this material, we subjected the free ligand ($HL5$) to reductive electrolysis in a $TBA^+BF_4^-$

supporting electrolyte, which is expected to form TBA^+L5^- with concomitant loss of H_2. Complete consumption of $HL5$ was confirmed by CV on the basis of the disappearance of the cathodic peak at −1.7 V (traces iv and v). CV of the species formed after bulk electrolysis shows a peak at −2.3 V, which we attribute to reduction of $L5^-$ to $L5^{2-}$. The corresponding oxidation of $L5^{2-}$ occurs at a much higher potential of −1.3 V. Most importantly, an additional irreversible peak is observed at positive potential (+0.5 V), likely corresponding to a $L5^-/L5^\bullet$ couple. This peak is the same as that observed in the CVs following cycling of the Zn and Mg MCCs. Furthermore, when a CV of $L5^-$ was measured with an identical voltage window to the MCCs, only the irreversible peak at +0.5 V was recorded (trace vi). Collectively, these data suggest that the oxidative peak observed after MCC decomposition results from oxidation of the free ligand $L5^-$ to neutral $L5^\bullet$, while oxidation of the neutral $HL5$ requires potentials beyond the measured CV window (trace iv).

These results provide evidence for the presence of free ligand in solution and thus support the hypothesis that ligand shedding plays a major role in MCC decomposition. The high stability of the neutral ML_2 complexes (stable for days at room temperature in CH_3CN without ligand loss) suggests that ligand shedding occurs from a reduced form of the MCC. To test this hypothesis, bulk electrolysis of $Mg(L5)_2$ was conducted without a voltaic cutoff while charging galvanostatically to $2e^-$ per molecule (Figure 5b). Charging curves during this experiment initially plateaued at −1.8 and −1.9 V, which correspond to the first and second reductions of $Mg(L5)_2$, respectively, but decreased to −2.3 V before complete charging
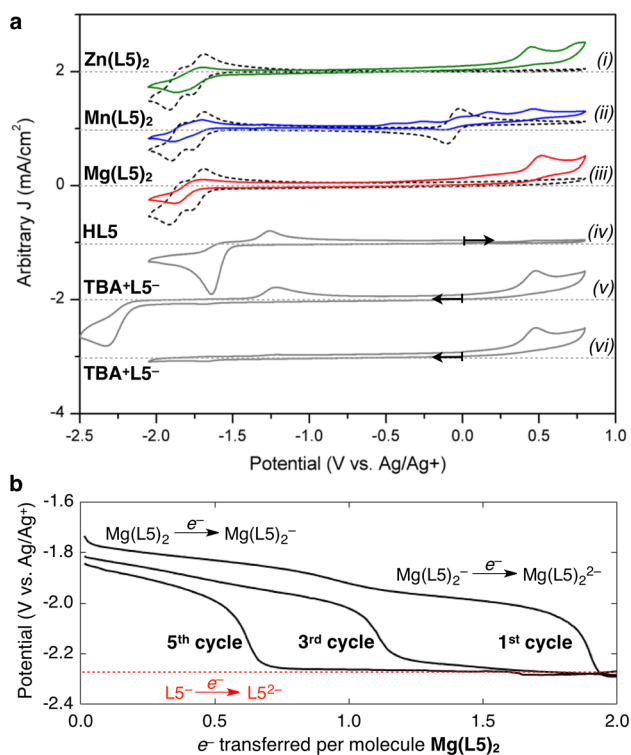
Figure 5. (a) CVs of unstable MCCs before (dashed, black traces) and after (solid, colored traces) cycling studies compared to free ligand. Gray dashed lines represent the axis of origin. Arrows denote the starting point and scanning direction. (b) Charging curves from electrolysis of a **Mg(L5)₂** solution.

through $2e^-$. This negative charging potential corresponds to the reduction of free ligand **L5⁻**, as revealed by CV trace v. The detection of free **L5⁻** within the short time frame of the first charging cycle (~10 min) indicates that decomposition to release free ligand occurs rapidly once **Mg(L5)₂** is reduced. Subsequent charging revealed that the complex continues to decompose and that electron transfer occurs primarily at the potential required for reduction of **L5⁻**.

An understanding of the decomposition mechanism and rate as a function of metal will guide the design of future generations of anolyte materials. Our cycling studies reveal that BPI complexes of Fe^{2+}, Co^{2+}, and Ni^{2+} are significantly more stable anolytes compared to those of Mg^{2+}, Mn^{2+}, and Zn^{2+}. The large effect of metal on stability was initially unexpected, given the similar CVs. In retrospect, we note that the observed trends for cycling stabilities of the $M(BPI)_2$ complexes correlate well with the rates of ligand exchange at divalent transition and main-group metals.[56] Metals with filled shells, such as Mg^{2+} or Zn^{2+}, lack ligand-field interactions, resulting in rapid rates of dissociative ligand substitution.[57] Conversely, metals with partially filled orbitals, such as Mn^{2+}, Fe^{2+}, Co^{2+}, or Ni^{2+}, form complexes that are far less susceptible to dissociative ligand substitution. However, unlike the complexes of the late transition metals, ligand substitution at many octahedral complexes of Mn^{2+} has been shown to occur predominantly by an *associative* mechanism.[58] As a result, the exchange of CH_3CN at $Mn(CH_3CN)_6^{2+}$ is 10 000 times faster than that at $Ni(CH_3CN)_6^{2+}$, and the rates of ligand exchange increase in the order $Ni^{2+} < Co^{2+} < Fe^{2+} \ll Mn^{2+}$.[56] Overall, our results highlight an inverse correlation between the rate of ligand exchange and stability during cycling. More generally,

because the predominant mechanisms of ligand substitution at different metals have been extensively studied,[56,59−61] these insights provide a guide to improve the electrochemical stability of a given MCC by targeting and inhibiting the known pathway for ligand exchange at that specific metal.

Extended Cycling and Shelf-Life Stability. We next conducted extended cycling studies to more thoroughly assess the optimal anolyte candidate. Our stability studies provided invaluable guidance in selecting the MCC for extended cycling. Ligand exchange at octahedral Ni^{2+} occurs with relatively slow rates via a dissociative mechanism, which suggests that $Ni(BPI)_2$ complexes should exhibit particularly high cycling stability. Thus, **Ni(L5)₂** was chosen for extended cycling to the commercial standard of 80% SOC.[62] The results from these studies are summarized in Figure 6a and demonstrate that this
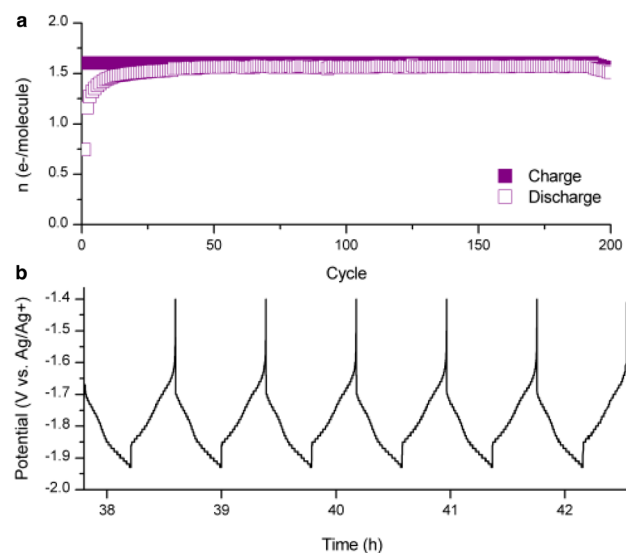

Figure 6. (a) Capacity retention of **Ni(L5)₂**. (b) Potential curves for cycles 100−105.

complex can be cycled through two electrons with <5% capacity fade after 200 cycles. Charge and discharge curves after 100 cycles, illustrated in Figure 6b, indicate that the **Ni(L5)₂** complex is charging through two couples at the expected potentials and discharging with high CE (97%).

In parallel with these multielectron cycling studies, we investigated the shelf-life stability of the charged MCC at high concentration. A 100 mM solution of **Ni(L6)₂** in CH_3CN was prepared with 0.5 M TBABF₄ supporting electrolyte.[63] This concentration is comparable to high concentration studies performed on NRFB chemistries in flow.[37,64] Galvanostatic charging of this solution was performed with a 50-fold greater current than the standard bulk-electrolysis experiments. The charging occurred at potentials that correlate well with the peaks observed by CV (−1.8, −2.0 V). An ohmic resistance contribution of 4 Ω was measured by electrochemical impedance spectroscopy. This is consistent with the low overpotentials observed during electrolysis. Once charged, the solution was removed from the H-cell and stored in a separate glass container under inert conditions at room temperature. The concentration of the charged MCC as a function of time was determined by CV. As plotted in Figure 7b, the doubly reduced MCC remained stable and soluble in the electrolyte solution for days at high concentration (0.1 M) without measurable degradation or precipitation.
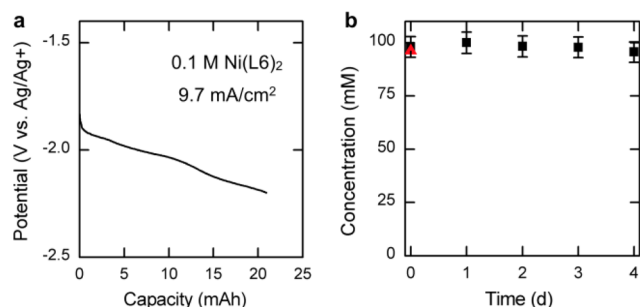
Figure 7. (a) Charging potential curve for a 2e⁻ reduction of a 100 mM solution of **Ni(L6)₂**. (b) Concentration of the charged **Ni(L6)₂** as a function of time. The red triangle represents the concentration of the neutral solution before cycling.

CONCLUSIONS

In summary, this paper describes the development of a series of MCCs containing earth-abundant metals and tridentate BPI ligands as potential anolyte materials for NRFBs. Systematic modification of the BPI ligand framework and the metal center enabled the identification of anolytes with high solubilities and low redox potentials. Studies of the decomposition of these complexes during bulk-electrolysis cycling revealed that ligand shedding is a major decomposition pathway. As such, we observe a strong correlation between MCC stability and the known rates of ligand substitution at divalent metal centers. Specifically, BPI complexes of nickel were found to undergo 200 charge and discharge cycles through two reductions with <5% capacity fade. Ultimately these studies led to the identification of **Ni(L6)₂**, a complex that possesses the previously unprecedented combination of high solubility, multiple electron transfers at low redox potentials, and high stability in the charged state, even at high concentration. Overall, the studies described herein have delivered a promising anolyte candidate for NRFBs and have also provided key insights into chemical design principles for future classes of MCC-based anolytes. Our ongoing work is focused on the design of second-generation complexes that address the remaining challenges associated with these materials. In particular, MCC-based anolytes with lower molecular weight per mole of electron transferred are important future targets.[54] Such materials should enable an increase in the effective concentration of the anolyte, thereby providing the high energy densities that are required for practical NRFB electrolytes.[54]

ASSOCIATED CONTENT

Ⓢ Supporting Information

The Supporting Information is available free of charge on the ACS Publications website at DOI: 10.1021/jacs.6b07638.

Crystallographic data of **Fe(L4)₂** in CIF format (CIF)
Crystallographic data of **HL4** in CIF format (CIF)
Crystallographic data of **Mn(L4)₂** in CIF format (CIF)
Crystallographic data of **Ni(L4)₂** in CIF format (CIF)
Crystallographic data of **Zn(L4)₂** in CIF format (CIF)
Experimental procedures and characterization of all new compounds, including spectroscopic data and potentiometric data (PDF)

AUTHOR INFORMATION

Corresponding Authors
*ltt@umich.edu
*mssanfor@umich.edu
Author Contributions
§C.S.S. and S.L.F. contributed equally to this work.
Notes
The authors declare no competing financial interest.

ACKNOWLEDGMENTS

REFERENCES

(1) Soloveichik, G. L. *Chem. Rev.* **2015**, *115*, 11533.
(2) Shin, S.-H.; Yun, S.-H.; Moon, S.-H. *RSC Adv.* **2013**, *3*, 9095.
(3) Wang, W.; Luo, Q.; Li, B.; Wei, X.; Li, L.; Yang, Z. *Adv. Funct. Mater.* **2013**, *23*, 970.
(4) Hou, Y.; Vidu, R.; Stroeve, P. *Ind. Eng. Chem. Res.* **2011**, *50*, 8954.
(5) Yang, Z.; Zhang, J.; Kintner-Meyer, M. C. W.; Lu, X.; Choi, D.; Lemmon, J. P.; Liu, J. *Chem. Rev.* **2011**, *111*, 3577.
(6) Sun, H.; Park, J. W.; Hwang, S. S.; Lee, D.; Lee, M. J. US Patent US8481192, 2013.
(7) Ding, C.; Zhang, H.; Li, X.; Liu, T.; Xing, F. *J. Phys. Chem. Lett.* **2013**, *4*, 1281.
(8) Winsberg, J.; Janoschka, T.; Morgenstern, S.; Hagemann, T.; Muench, S.; Hauffman, G.; Gohy, J.-F.; Hager, M. D.; Schubert, U. S. *Adv. Mater.* **2016**, *28*, 2238.
(9) Janoschka, T.; Martin, N.; Martin, U.; Friebe, C.; Morgenstern, S.; Hiller, H.; Hager, M. D.; Schubert, U. S. *Nature* **2015**, *527*, 78.
(10) Janoschka, T.; Hager, M. D.; Schubert, U. S. *Adv. Mater.* **2012**, *24*, 6397.
(11) Lin, K.; Chen, Q.; Gerhardt, M. R.; Tong, L.; Kim, S. B.; Eisenach, L.; Valle, A. W.; Hardee, D.; Gordon, R. G.; Aziz, M. J.; Marshak, M. P. *Science* **2015**, *349*, 1529.
(12) Huskinson, B.; Marshak, M. P.; Suh, C.; Er, S.; Gerhardt, M. R.; Galvin, C. J.; Chen, X.; Aspuru-Guzik, A.; Gordon, R. G.; Aziz, M. J. *Nature* **2014**, *505*, 195.
(13) Liu, T.; Wei, X.; Nie, Z.; Sprenkle, V.; Wang, W. *Adv. Energy Mater.* **2016**, *6*, 1501449.
(14) Darling, R. M.; Weber, A. Z.; Tucker, M. C.; Perry, M. L. *J. Electrochem. Soc.* **2016**, *163*, A5014.
(15) Darling, R.; Gallagher, K.; Xie, W.; Su, L.; Brushett, F. *J. Electrochem. Soc.* **2016**, *163*, A5029.
(16) Su, L.; Darling, R. M.; Gallagher, K. G.; Xie, W.; Thelen, J. L.; Badel, A. F.; Barton, J. L.; Cheng, K. J.; Balsara, N. P.; Moore, J. S.; Brushett, F. R. *J. Electrochem. Soc.* **2016**, *163*, A5253.
(17) Nagarjuna, G.; Hui, J.; Cheng, K. J.; Lichtenstein, T.; Shen, M.; Moore, J. S.; Rodríguez-López, J. *J. Am. Chem. Soc.* **2014**, *136*, 16309.
(18) Zhang, D.; Lan, H.; Li, Y. *J. Power Sources* **2012**, *217*, 199.
(19) Liu, Q.; Sleightholme, A. E. S.; Shinkle, A. A.; Li, Y.; Thompson, L. T. *Electrochem. Commun.* **2009**, *11*, 2312.
(20) Sleightholme, A. E. S.; Shinkle, A. A.; Liu, Q.; Li, Y.; Monroe, C. W.; Thompson, L. T. *J. Power Sources* **2011**, *196*, 5742.
(21) Yamamura, T.; Shiokawa, Y.; Yamana, H.; Moriyama, H. *Electrochim. Acta* **2002**, *48*, 43.
(22) Suttil, J. A.; Kucharyson, J. F.; Escalante-Garcia, I. L.; Cabrera, P. J.; James, B. R.; Savinell, R. F.; Sanford, M. S.; Thompson, L. T. *J. Mater. Chem. A* **2015**, *3*, 7929.
(23) Eisenberg, R.; Gray, H. B. *Inorg. Chem.* **2011**, *50*, 9741.
(24) Cappillino, P. J.; Pratt, H. D.; Hudak, N. S.; Tomson, N. C.; Anderson, T. M.; Anstey, M. R. *Adv. Energy Mater.* **2014**, *4*, 1300566.
(25) Xing, X.; Zhang, D.; Li, Y. *J. Power Sources* **2015**, *279*, 205.

(26) Park, M.-S.; Lee, N.-J.; Lee, S.-W.; Kim, K. J.; Oh, D.-J.; Kim, Y.-J. *ACS Appl. Mater. Interfaces* **2014**, *6*, 10729.

(27) Chakrabarti, M. H.; Dryfe, R. A. W.; Roberts, E. P. L. *Electrochim. Acta* **2007**, *52*, 2189.

(28) Chakrabarti, M. H.; Lindfield Roberts, E. P.; Saleem, M. *Int. J. Green Energy* **2010**, *7*, 445.

(29) Morita, M.; Tanaka, Y.; Tanaka, K.; Matsuda, Y.; Matsumura-Inoue, T. *Bull. Chem. Soc. Jpn.* **1988**, *61*, 2711.

(30) Matsuda, Y.; Tanaka, K.; Okada, M.; Takasu, Y.; Morita, M.; Matsumura-Inoue, T. *J. Appl. Electrochem.* **1988**, *18*, 909.

(31) Mun, J.; Lee, M.-J.; Park, J.-W.; Oh, D.-J.; Lee, D.-Y.; Doo, S.-G. *Electrochem. Solid-State Lett.* **2012**, *15*, A80.

(32) Kim, J.-H.; Kim, K. J.; Park, M.-S.; Lee, N. J.; Hwang, U.; Kim, H.; Kim, Y.-J. *Electrochem. Commun.* **2011**, *13*, 997.

(33) Cabrera, P. J.; Yang, X.; Suttil, J. A.; Brooner, R. E. M.; Thompson, L. T.; Sanford, M. S. *Inorg. Chem.* **2015**, *54*, 10214.

(34) Cabrera, P. J.; Yang, X.; Suttil, J. A.; Hawthorne, K. L.; Brooner, R. E. M.; Sanford, M. S.; Thompson, L. T. *J. Phys. Chem. C* **2015**, *119*, 15882.

(35) Zhao, Y.; Ding, Y.; Song, J.; Li, G.; Dong, G.; Goodenough, J. B.; Yu, G. *Angew. Chem., Int. Ed.* **2014**, *53*, 11036.

(36) Hwang, B.; Park, M.-S.; Kim, K. *ChemSusChem* **2015**, *8*, 310.

(37) Wei, X. L.; Cosimbescu, L.; Xu, W.; Hu, J. Z.; Vijayakumar, M.; Feng, J.; Hu, M. Y.; Deng, X. C.; Xiao, J.; Liu, J.; Sprenkle, V.; Wang, W. *Adv. Energy Mater.* **2015**, *5*, 1400678.

(38) Escalante-García, I. L.; Wainright, J. S.; Thompson, L. T.; Savinell, R. F. *J. Electrochem. Soc.* **2015**, *162*, A363.

(39) Liu, Q.; Shinkle, A. A.; Li, Y.; Monroe, C. W.; Thompson, L. T.; Sleightholme, A. E. S. *Electrochem. Commun.* **2010**, *12*, 1634.

(40) Shinkle, A. A.; Sleightholme, A. E. S.; Griffith, L. D.; Thompson, L. T.; Monroe, C. W. *J. Power Sources* **2012**, *206*, 490.

(41) Nawi, M. A.; Riechel, T. L. *Inorg. Chem.* **1981**, *20*, 1974.

(42) Kitamura, M.; Yamashita, K.; Imai, H. *Bull. Chem. Soc. Jpn.* **1976**, *49*, 97.

(43) Csonka, R.; Speier, G.; Kaizer, J. *RSC Adv.* **2015**, *5*, 18401.

(44) Gagne, R. R.; Marritt, W. A.; Marks, D. N.; Siegl, W. O. *Inorg. Chem.* **1981**, *20*, 3260.

(45) Freeman, D. H.; Swahn, I. D.; Hambright, P. *Energy Fuels* **1990**, *4*, 699.

(46) Huang, X. F.; Nakanishi, K.; Berova, N. *Chirality* **2000**, *12*, 237.

(47) Ozaki, S.; Nakagawa, Y.; Shirai, O.; Kano, K. *J. Pharm. Sci.* **2014**, *103*, 3524.

(48) Docherty, R.; Pencheva, K.; Abramov, Y. A. *J. Pharm. Pharmacol.* **2015**, *67*, 847.

(49) Takeuchi, T.; Oishi, S.; Kaneda, M.; Ohno, H.; Nakamura, S.; Nakanishi, I.; Yamane, M.; Sawada, J.-i.; Asai, A.; Fujii, N. *ACS Med. Chem. Lett.* **2014**, *5*, 566.

(50) Ishikawa, M.; Hashimoto, Y. *J. Med. Chem.* **2011**, *54*, 1539.

(51) This is the maximum concentration of a two-electron anolyte that could be electrochemically supported by the given electrolyte stoichiometry.

(52) Teoh, W. H.; Mammucari, R.; Foster, N. R. *J. Organomet. Chem.* **2013**, *724*, 102.

(53) Aschenbrenner, O.; Kemper, S.; Dahmen, N.; Schaber, K.; Dinjus, E. *J. Supercrit. Fluids* **2007**, *41*, 179.

(54) Darling, R. M.; Gallagher, K. G.; Kowalski, J. A.; Ha, S.; Brushett, F. R. *Energy Environ. Sci.* **2014**, *7*, 3459.

(55) Oxidation of Mg(II) or Zn(II) is unlikely to occur at such low potentials.

(56) Helm, L.; Merbach, A. E. *Chem. Rev.* **2005**, *105*, 1923.

(57) Nakamura, S.; Meiboom, S. *J. Am. Chem. Soc.* **1967**, *89*, 1765.

(58) Inada, Y.; Sugata, T.; Ozutsumi, K.; Funahashi, S. *Inorg. Chem.* **1998**, *37*, 1886.

(59) Lincoln, S. F.; Merbach, A. E. In *Advances in Inorganic Chemistry*; Sykes, A. G., Ed.; Academic Press, 1995; Vol. *42*, p 1.

(60) Hogg, R.; Wilkins, R. G. *J. Chem. Soc.* **1962**, *0*, 341.

(61) Holyer, R. H.; Hubbard, C. D.; Kettle, S. F. A.; Wilkins, R. G. *Inorg. Chem.* **1965**, *4*, 929.

(62) Li, L.; Kim, S.; Wang, W.; Vijayakumar, M.; Nie, Z.; Chen, B.; Zhang, J.; Xia, G.; Hu, J.; Graff, G.; Liu, J.; Yang, Z. *Adv. Energy Mater.* **2011**, *1*, 394.

(63) Because this complex undergoes two reversible reductions, it has twice the storage capacity of a one-electron anolyte. As such, a 100 mM solution is equivalent to reduction of a 200 mM solution containing a one-electron anolyte.

(64) Wei, X.; Xu, W.; Vijayakumar, M.; Cosimbescu, L.; Liu, T.; Sprenkle, V.; Wang, W. *Adv. Mater.* **2014**, *26*, 7649.